

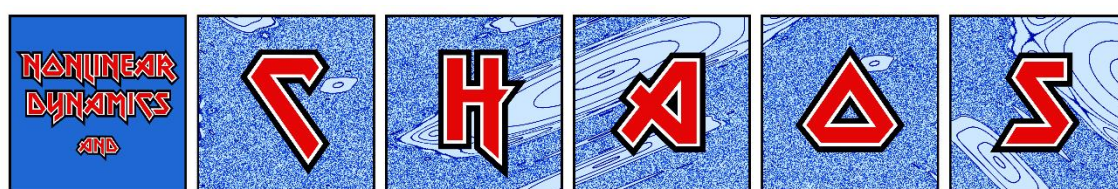
Quantifying chaos using Lagrangian descriptors

Haris Skokos

**Nonlinear Dynamics and Chaos (NDC) group
Department of Mathematics and Applied Mathematics
University of Cape Town, South Africa**

**E-mail: haris.skokos@uct.ac.za, haris.skokos@gmail.com
URL: http://math_research.uct.ac.za/~hskokos/**

**International Conference on Nonlinear Science and Complexity
Yibin, China, 5 August 2024**



Outline

- **Lagrangian descriptors (LDs)**
- **Smaller Alignment Index (SALI)**
- **Chaos diagnostics based on LDs:**
 - ✓ **the difference of LDs of neighboring orbits**
 - ✓ **the ratio of LDs of neighboring orbits**
 - ✓ **a quantity related to the finite-difference second spatial derivative of LDs**
- **Applications:**
 - ✓ **Hénon – Heiles system**
 - ✓ **2D Standard map**
 - ✓ **4D Standard map**
- **Summary**

Lagrangian descriptors (LDs)

The computation of LDs is based on the accumulation of some positive scalar value along the path of individual orbits.

Consider an N dimensional continuous time dynamical system

$$\dot{\mathbf{x}} = \frac{d\mathbf{x}(t)}{dt} = \mathbf{f}(\mathbf{x}, t)$$

The Arclength Definition [Madrid & Mancho, Chaos (2009) – Mendoza & Mancho, PRL (2010) – Mancho et al., Commun. Nonlin. Sci. Num. Simul. (2013)].

Forward time LD:

$$LD^f(\mathbf{x}, \tau) = \int_0^\tau \|\dot{\mathbf{x}}(t)\| dt$$

Backward time LD:

$$LD^b(\mathbf{x}, \tau) = \int_{-\tau}^0 \|\dot{\mathbf{x}}(t)\| dt$$

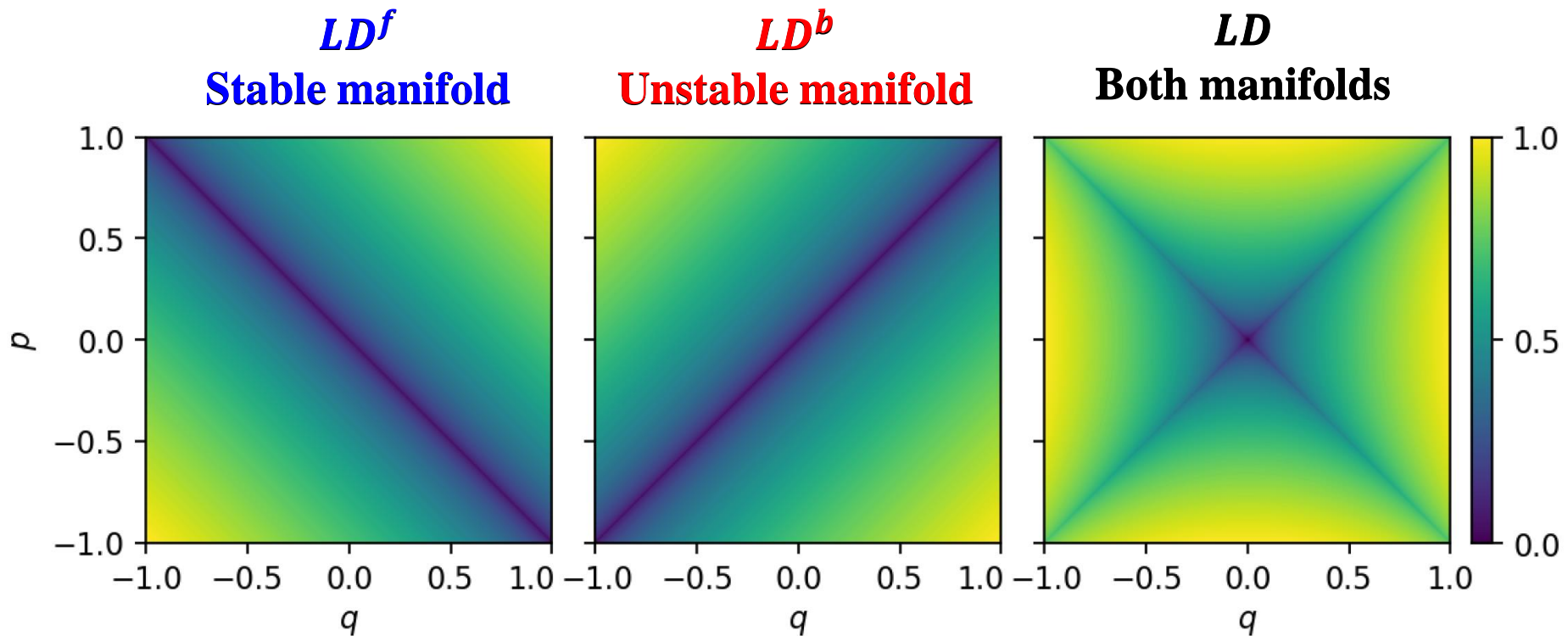
Combined LD:

$$LD(\mathbf{x}, \tau) = LD^b(\mathbf{x}, \tau) + LD^f(\mathbf{x}, \tau)$$

LDs: 1 degree of freedom (dof) Hamiltonian

$$H(q, p) = \frac{1}{2} (p^2 - q^2)$$

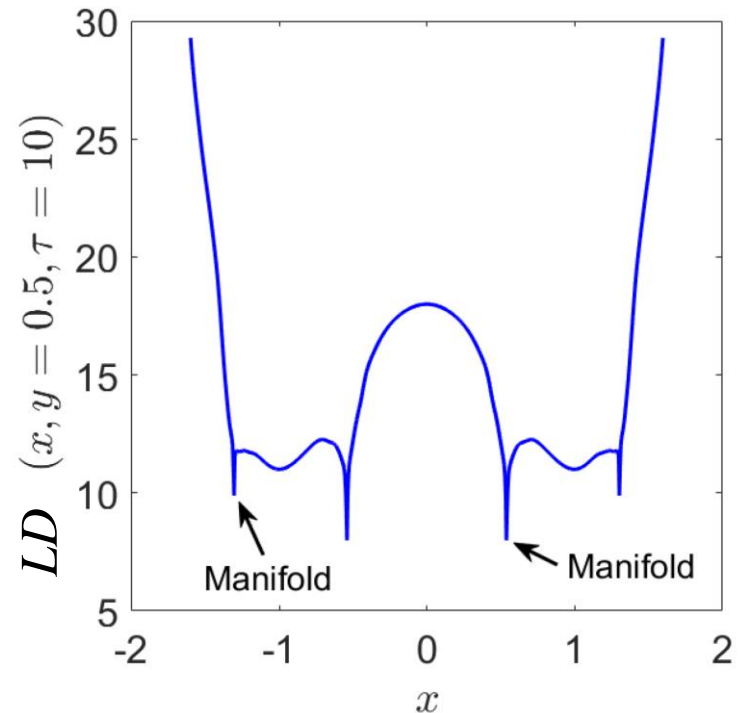
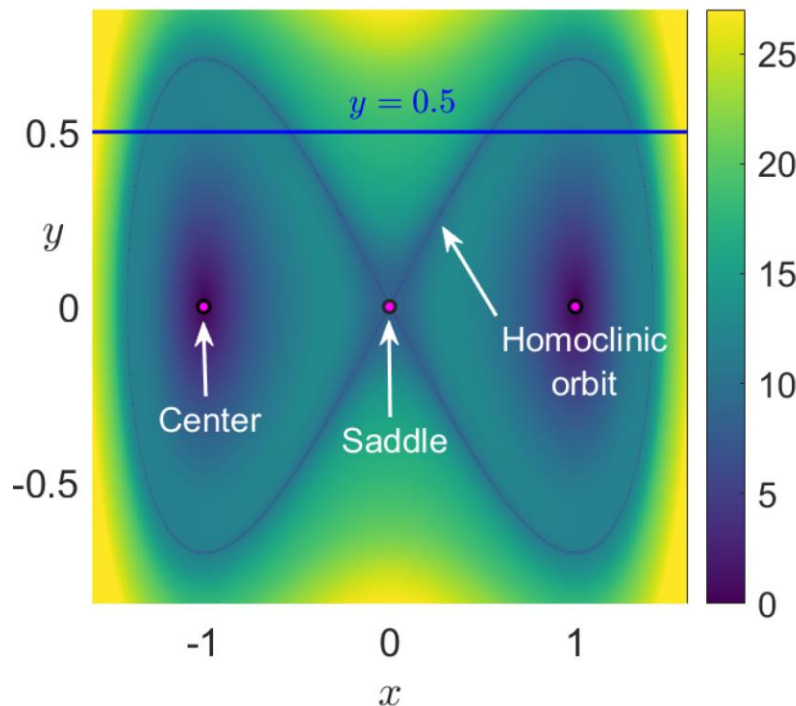
The system has a hyperbolic fixed point at the origin. The LDs can be used to display the stable and unstable manifolds of this point.



LDs: 1 dof Duffing Oscillator

$$H(x, y) = \frac{1}{2}y^2 + \frac{1}{4}x^4 - \frac{1}{2}x^2$$

The system has three equilibrium points: a saddle located at the origin and two diametrically opposed centers at the points $(\pm 1, 0)$.



From Agaoglou et al. 'Lagrangian descriptors: Discovery and quantification of phase space structure and transport', 2020, <https://doi.org/10.5281/zenodo.3958985>

The **location of the stable and unstable manifolds** can be extracted from the ridges of the **gradient field of the LDs** since they are located at points where the forward and the backward components of the LD are non-differentiable.

Lagrangian descriptors (LDs)

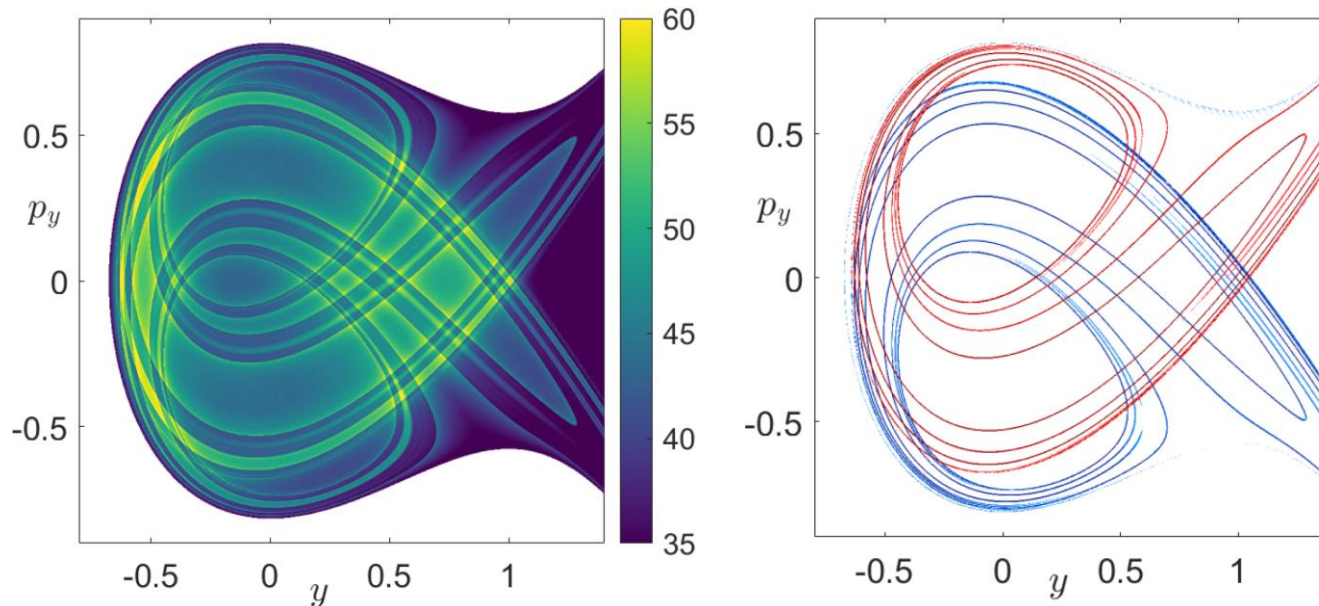
The ‘ p -norm’ Definition [Lopesino et al., Commun. Nonlin. Sci. Num. Simul. (2015) – Lopesino et al., Int. J. Bifurc. Chaos (2017)].

Combined LD (usually $p=1/2$):

$$LD(x, \tau) = \int_{-\tau}^{\tau} \left(\sum_{i=1}^N |f_i(x, t)|^p \right) dt$$

Hénon-Heiles system: $H = \frac{1}{2}(p_x^2 + p_y^2) + \frac{1}{2}(x^2 + y^2) + x^2y - \frac{1}{3}y^3$

Stable and **unstable** manifolds for $H=1/3$, $\tau=10$.



Maximum Lyapunov Exponent (MLE)

Chaos: sensitive dependence on initial conditions.

Roughly speaking, the MLE of a given orbit characterizes the **mean exponential rate of divergence** of trajectories surrounding it.

Consider an orbit in the $2N$ -dimensional phase space with **initial condition $\mathbf{x}(0)$** and **an initial deviation vector (small perturbation) from it $\mathbf{v}(0)$** .

Then the mean exponential rate of divergence is:

$$\text{MLE} = \lambda_1 = \lim_{t \rightarrow \infty} \Lambda(t) = \lim_{t \rightarrow \infty} \frac{1}{t} \ln \frac{\|\mathbf{v}(t)\|}{\|\mathbf{v}(0)\|}$$

$\lambda_1 = 0 \rightarrow$ Regular motion ($\Lambda \propto t^{-1}$)

$\lambda_1 > 0 \rightarrow$ Chaotic motion

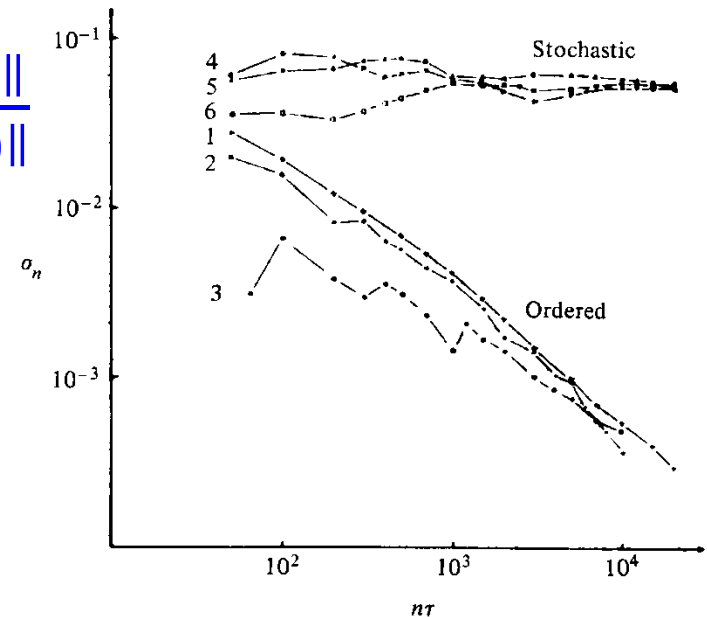


Figure 5.7. Behavior of σ_n at the intermediate energy $E = 0.125$ for initial points taken in the ordered (curves 1–3) or stochastic (curves 4–6) regions (after Benettin *et al.*, 1976).

The Smaller Alignment Index (SALI)

Consider the **2N-dimensional phase space** of a conservative dynamical system (**symplectic map or Hamiltonian flow**).

An orbit in that space with initial condition :

$$P(\mathbf{0})=(x_1(\mathbf{0}), x_2(\mathbf{0}), \dots, x_{2N}(\mathbf{0}))$$

and a **deviation vector**

$$v(\mathbf{0})=(\delta x_1(\mathbf{0}), \delta x_2(\mathbf{0}), \dots, \delta x_{2N}(\mathbf{0}))$$

The evolution in time (in maps the time is discrete and is equal to the number n of the iterations) of a **deviation vector** is defined by:

- the **variational equations** (for Hamiltonian flows) and
- the equations of the **tangent map** (for mappings)

Definition of the SALI

We follow the evolution in time of two different initial deviation vectors ($v_1(0)$, $v_2(0)$), and define SALI [S., J. Phys. A (2001) – S & Manos, Lect. Notes Phys. (2016)] as:

$$\text{SALI}(t) = \min\{\|\hat{v}_1(t) + \hat{v}_2(t)\|, \|\hat{v}_1(t) - \hat{v}_2(t)\|\}$$

where

$$\hat{v}_1(t) = \frac{v_1(t)}{\|v_1(t)\|}$$

When the two vectors become collinear

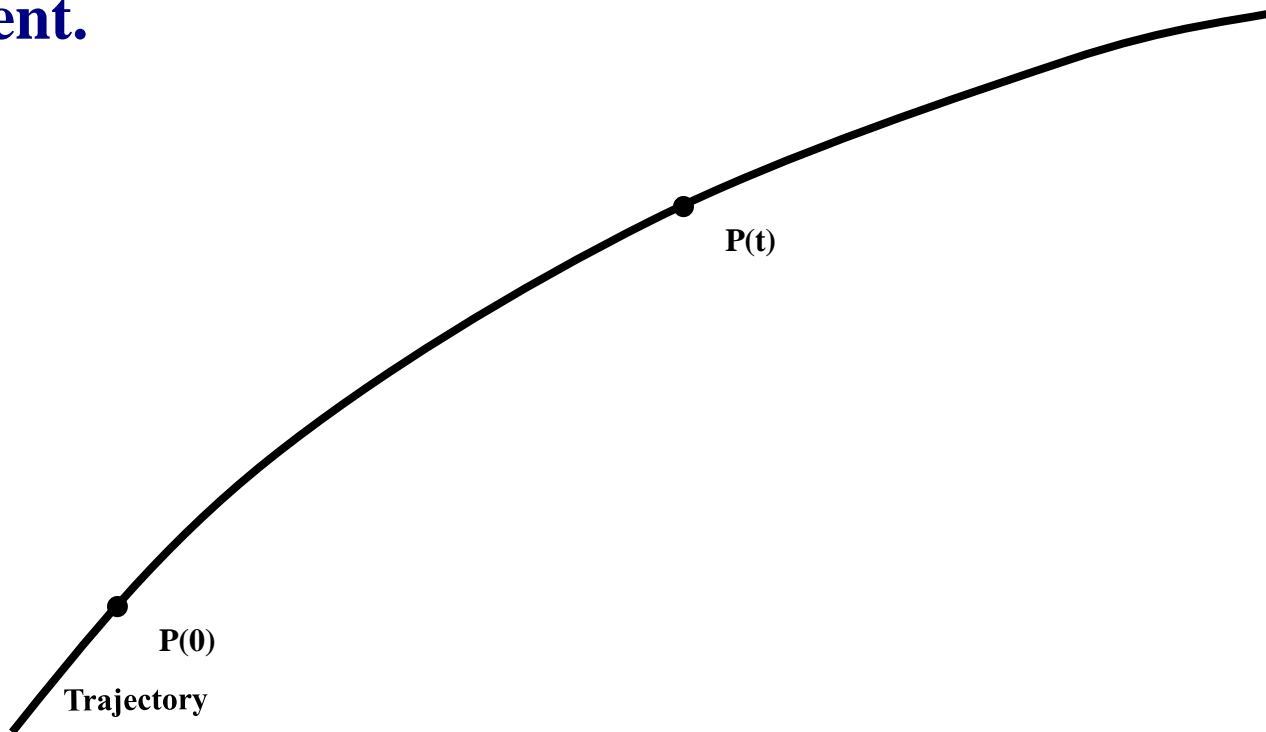
$$\text{SALI}(t) \rightarrow 0$$

Behavior of SALI for chaotic motion

For chaotic orbits the two initially different deviation vectors tend to coincide with the direction defined by the maximum Lyapunov exponent.

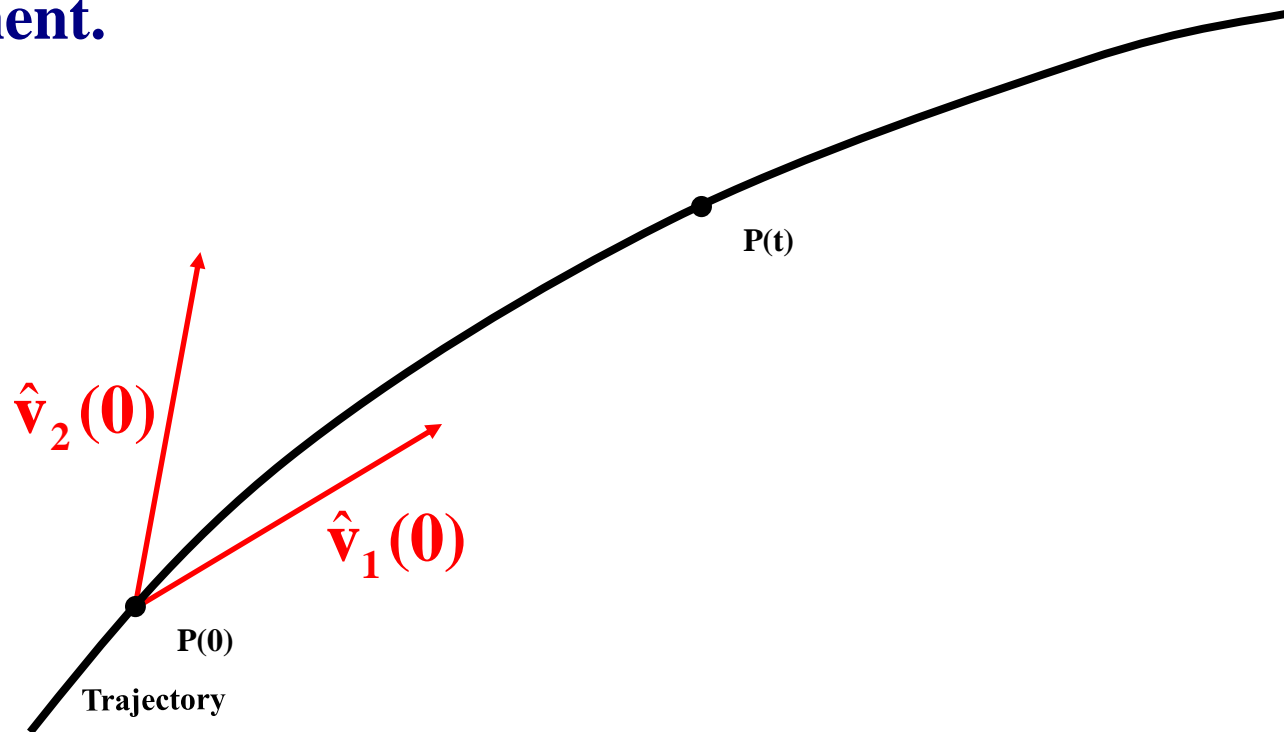
Behavior of SALI for chaotic motion

For chaotic orbits the two initially different deviation vectors tend to coincide with the direction defined by the maximum Lyapunov exponent.



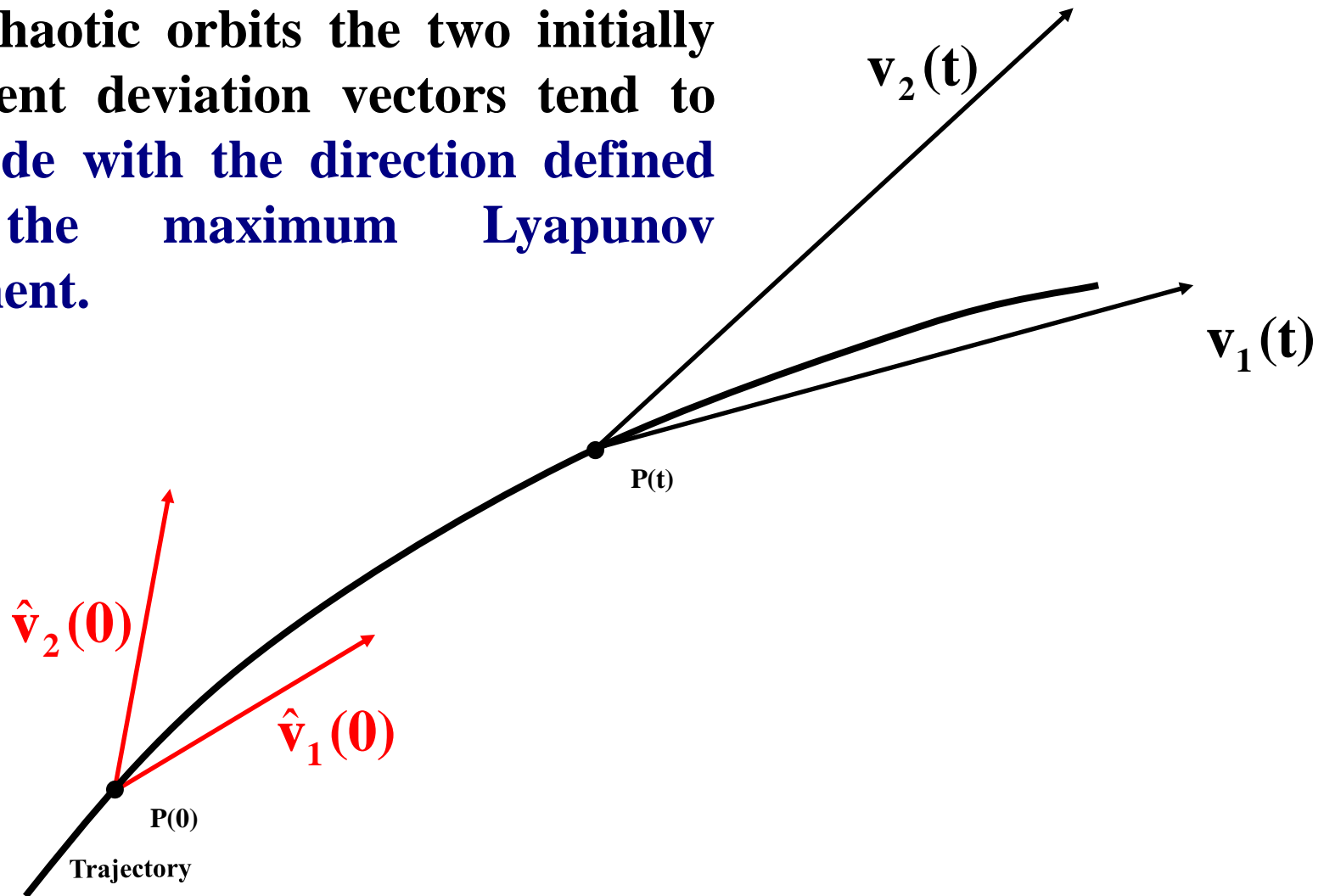
Behavior of SALI for chaotic motion

For chaotic orbits the two initially different deviation vectors tend to coincide with the direction defined by the maximum Lyapunov exponent.



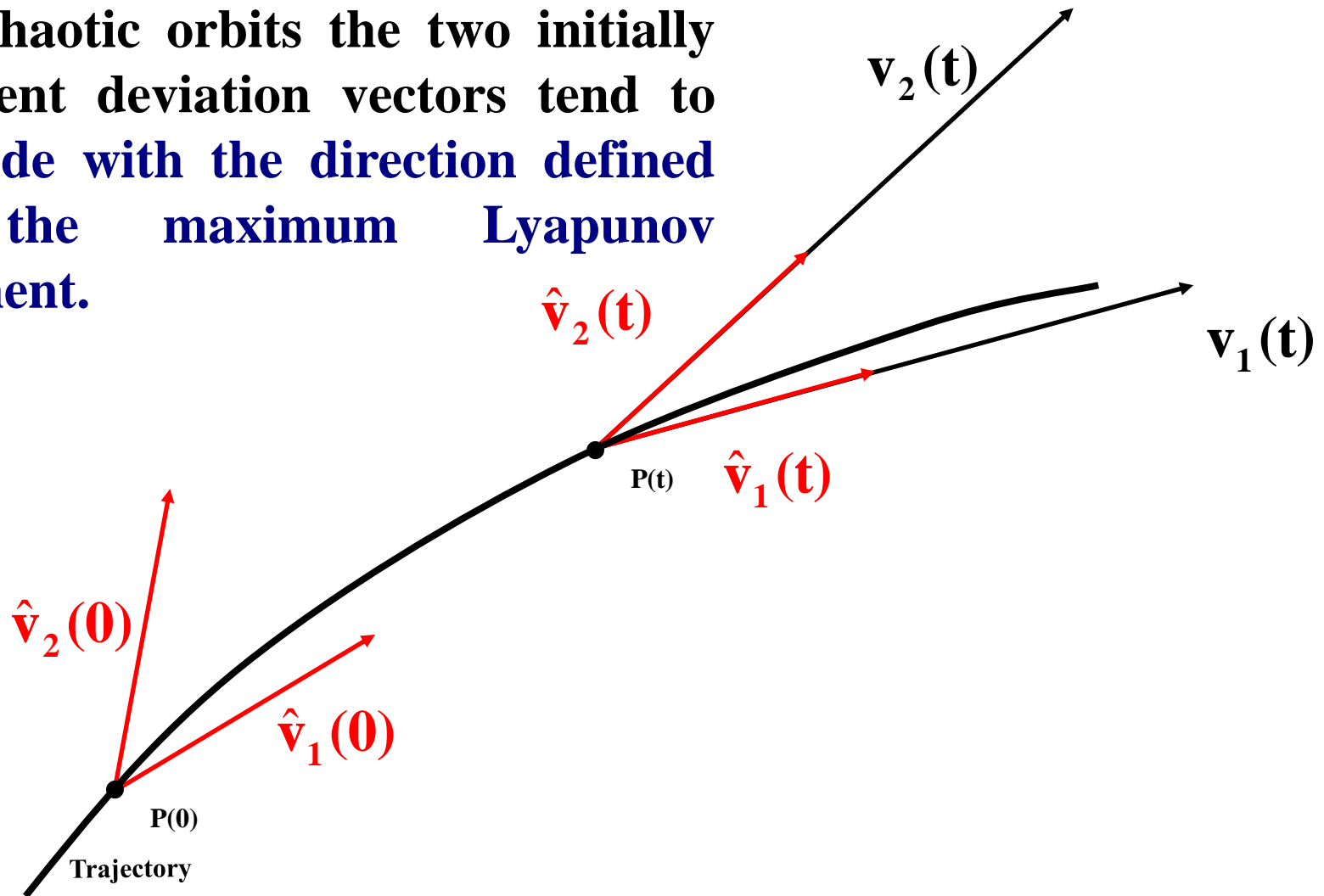
Behavior of SALI for chaotic motion

For chaotic orbits the two initially different deviation vectors tend to coincide with the direction defined by the maximum Lyapunov exponent.



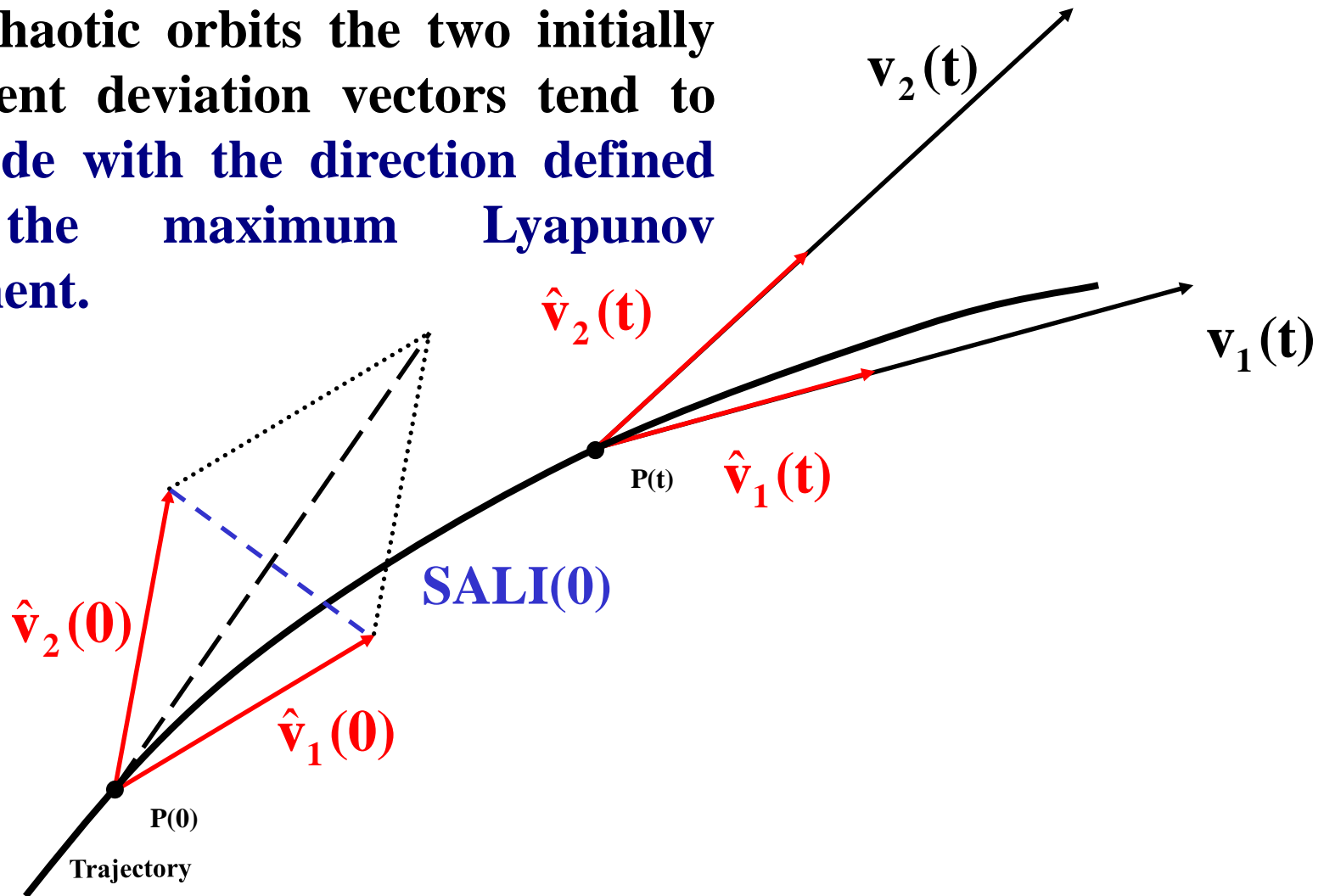
Behavior of SALI for chaotic motion

For chaotic orbits the two initially different deviation vectors tend to coincide with the direction defined by the maximum Lyapunov exponent.



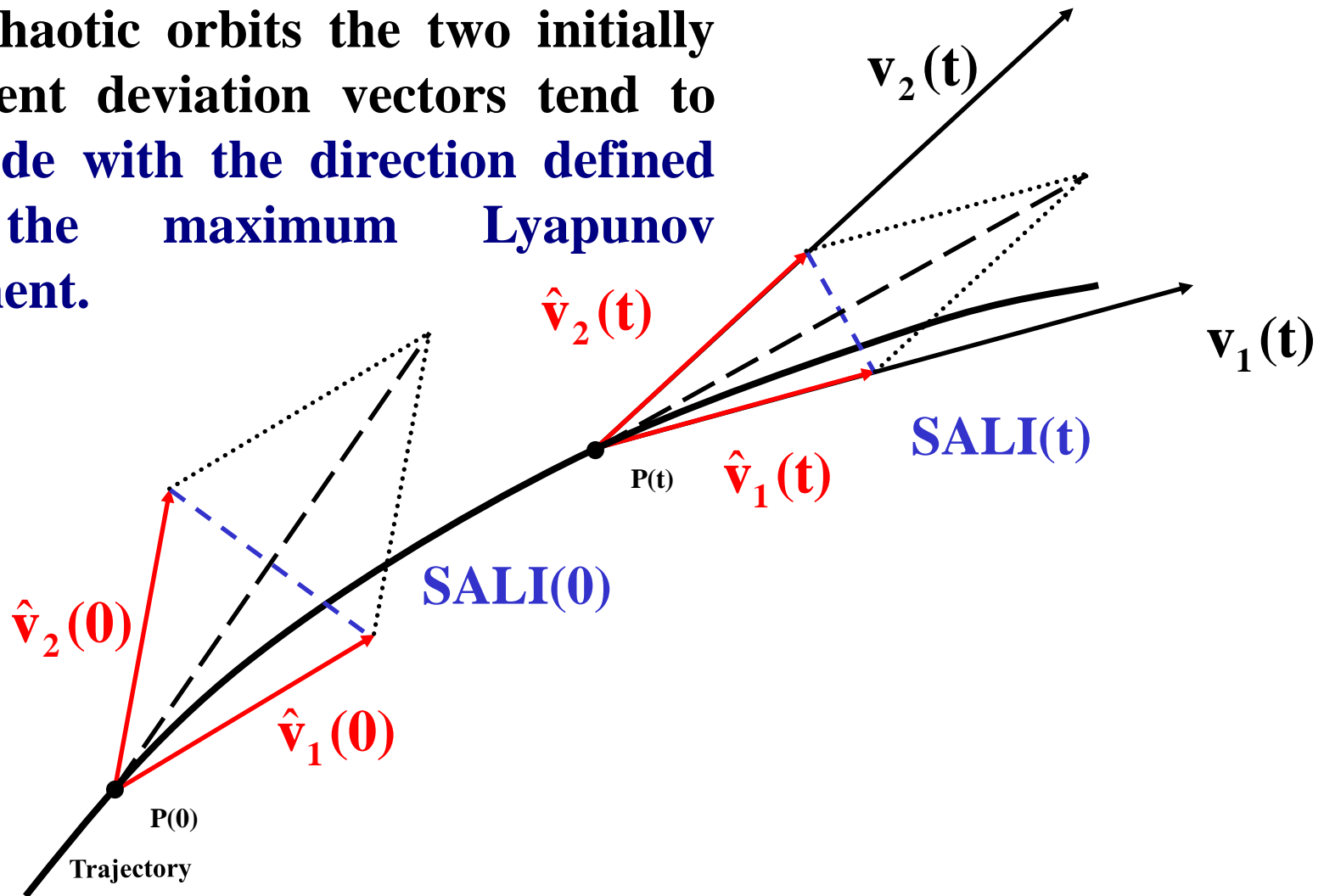
Behavior of SALI for chaotic motion

For chaotic orbits the two initially different deviation vectors tend to coincide with the direction defined by the maximum Lyapunov exponent.



Behavior of SALI for chaotic motion

For chaotic orbits the two initially different deviation vectors tend to coincide with the direction defined by the maximum Lyapunov exponent.

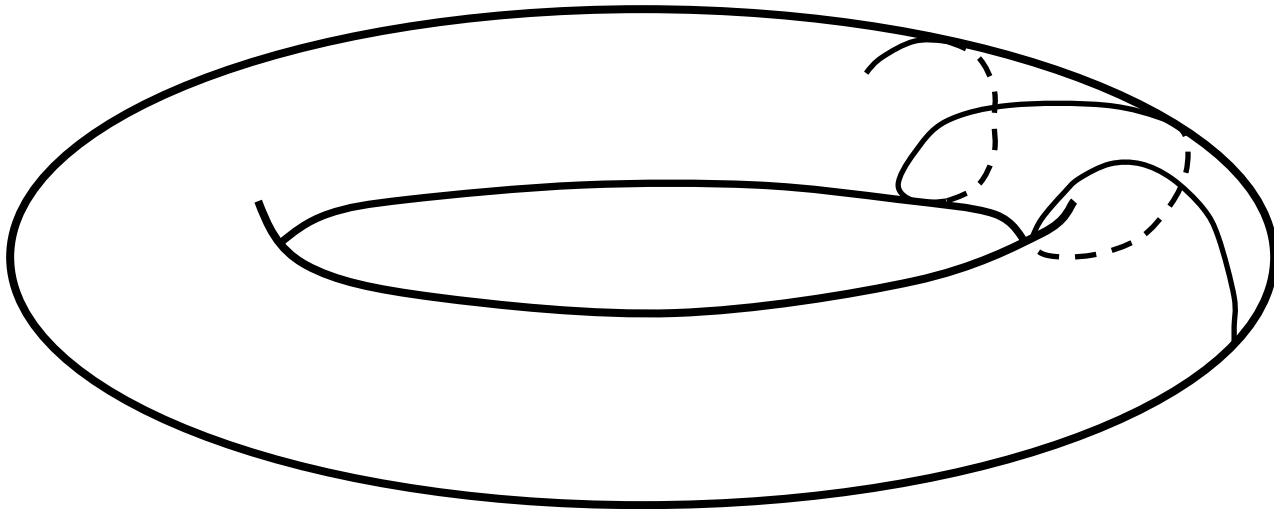


Behavior of SALI for regular motion

Regular motion occurs on a torus and two different initial deviation vectors become tangent to the torus, generally having different directions.

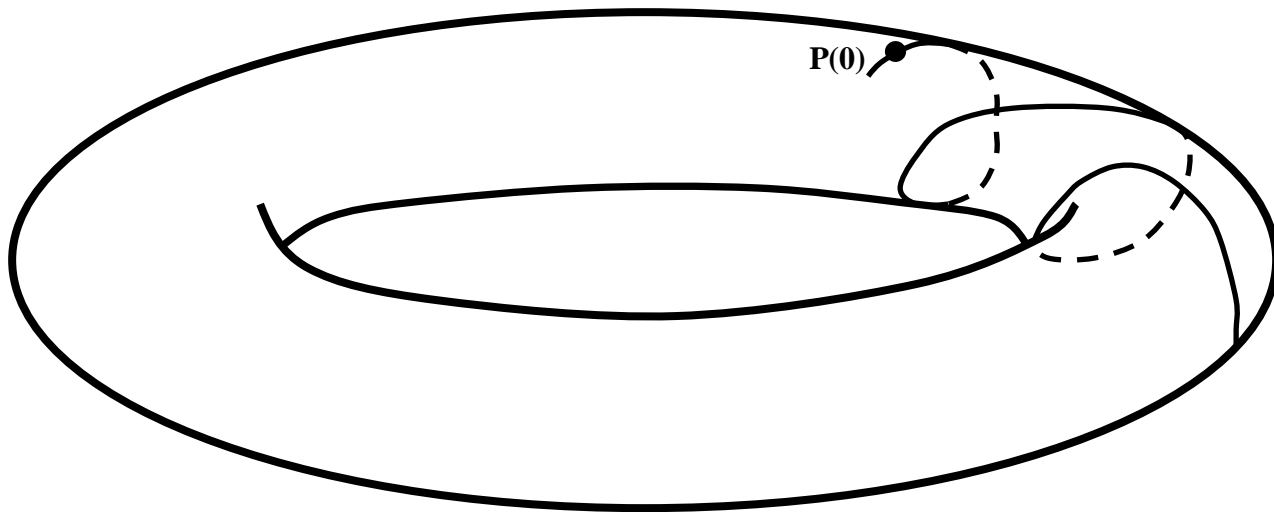
Behavior of SALI for **regular motion**

Regular motion occurs on a torus and two different initial deviation vectors **become tangent to the torus, generally having different directions.**



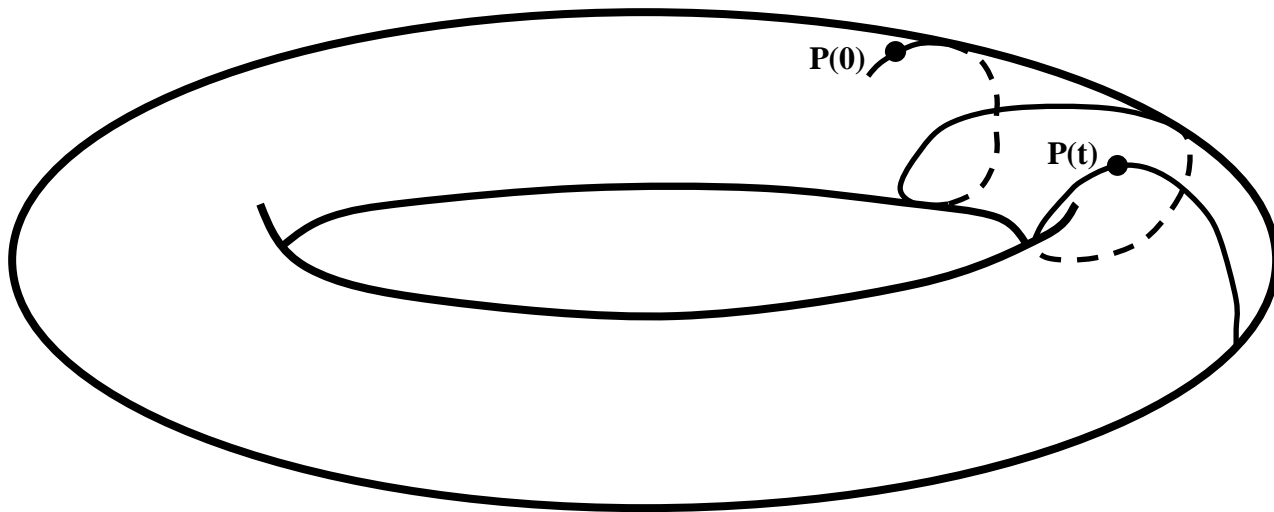
Behavior of SALI for **regular motion**

Regular motion occurs on a torus and two different initial deviation vectors **become tangent to the torus, generally having different directions.**



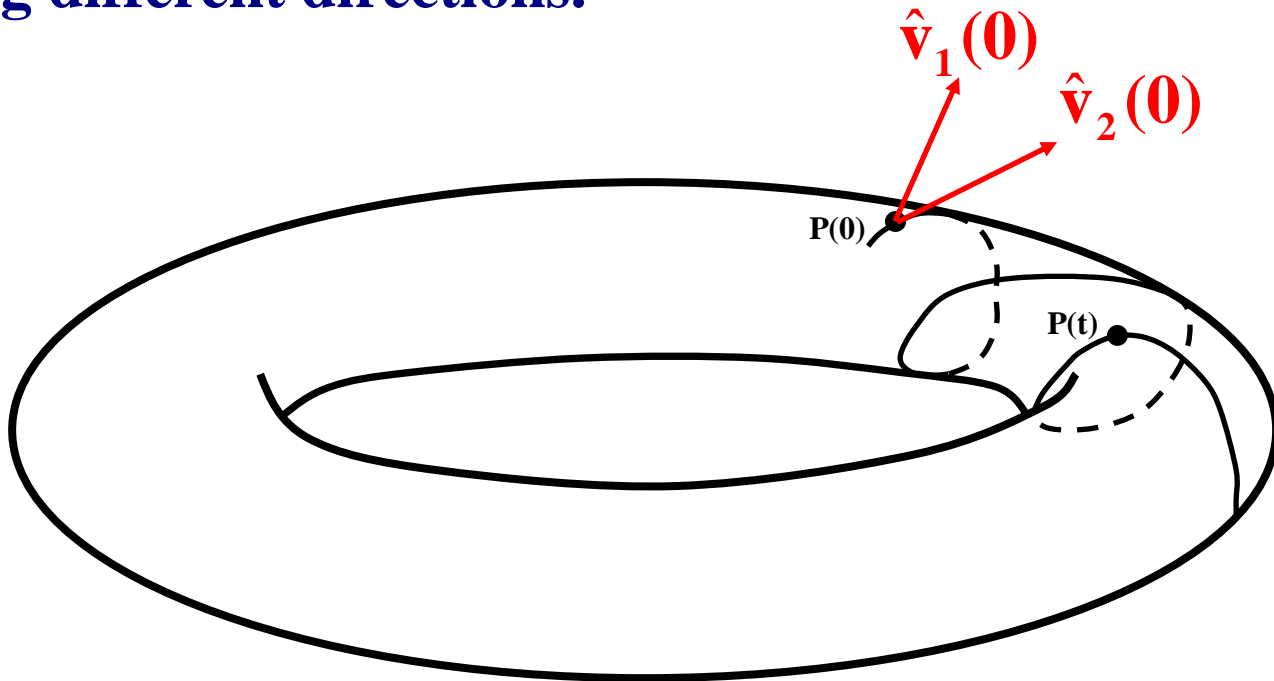
Behavior of SALI for **regular motion**

Regular motion occurs on a torus and two different initial deviation vectors **become tangent to the torus, generally having different directions.**



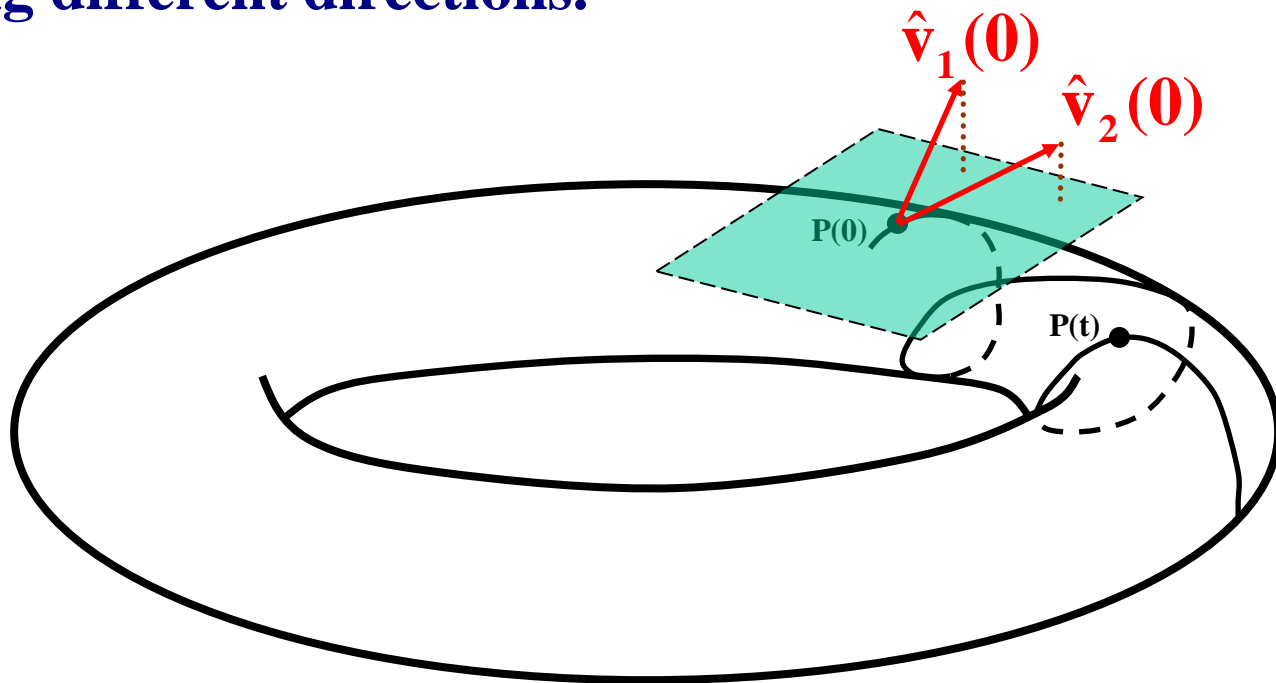
Behavior of SALI for **regular motion**

Regular motion occurs on a torus and two different initial deviation vectors **become tangent to the torus, generally having different directions.**



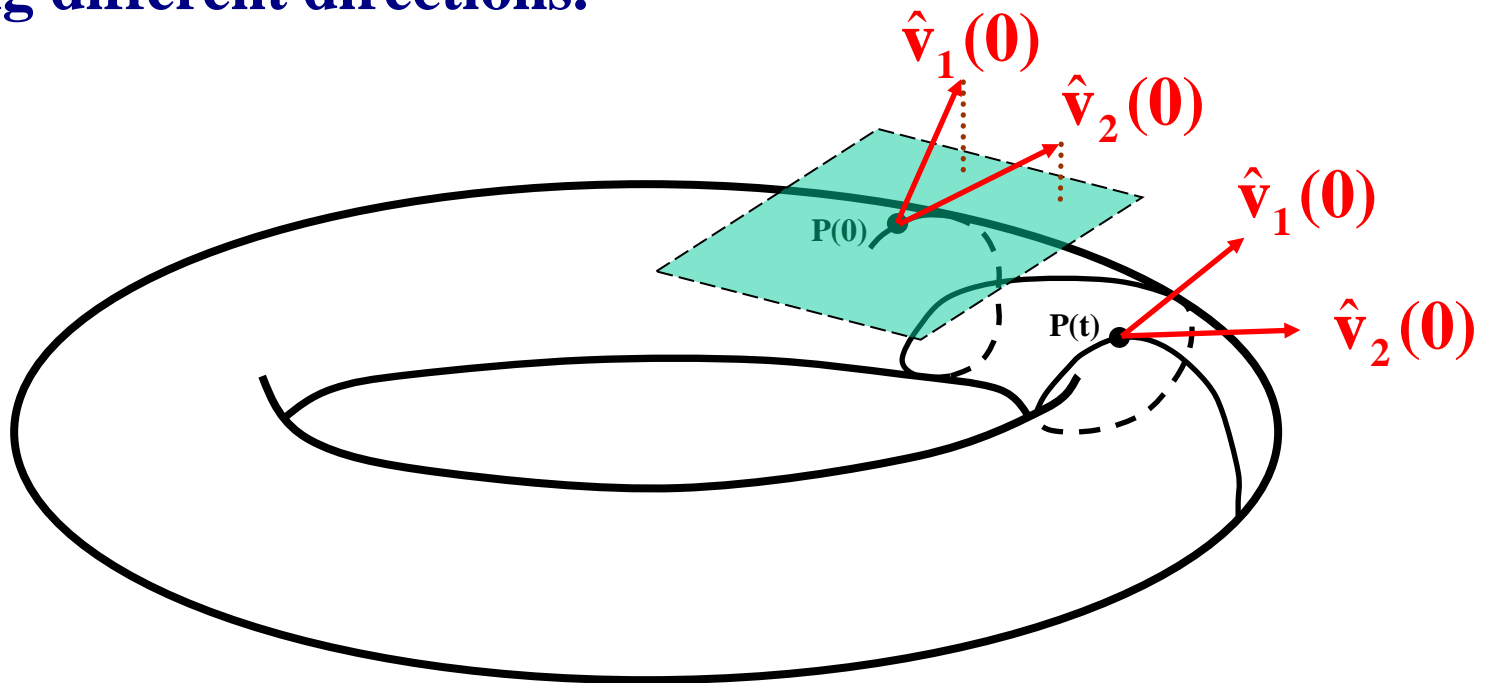
Behavior of SALI for regular motion

Regular motion occurs on a torus and two different initial deviation vectors become tangent to the torus, generally having different directions.



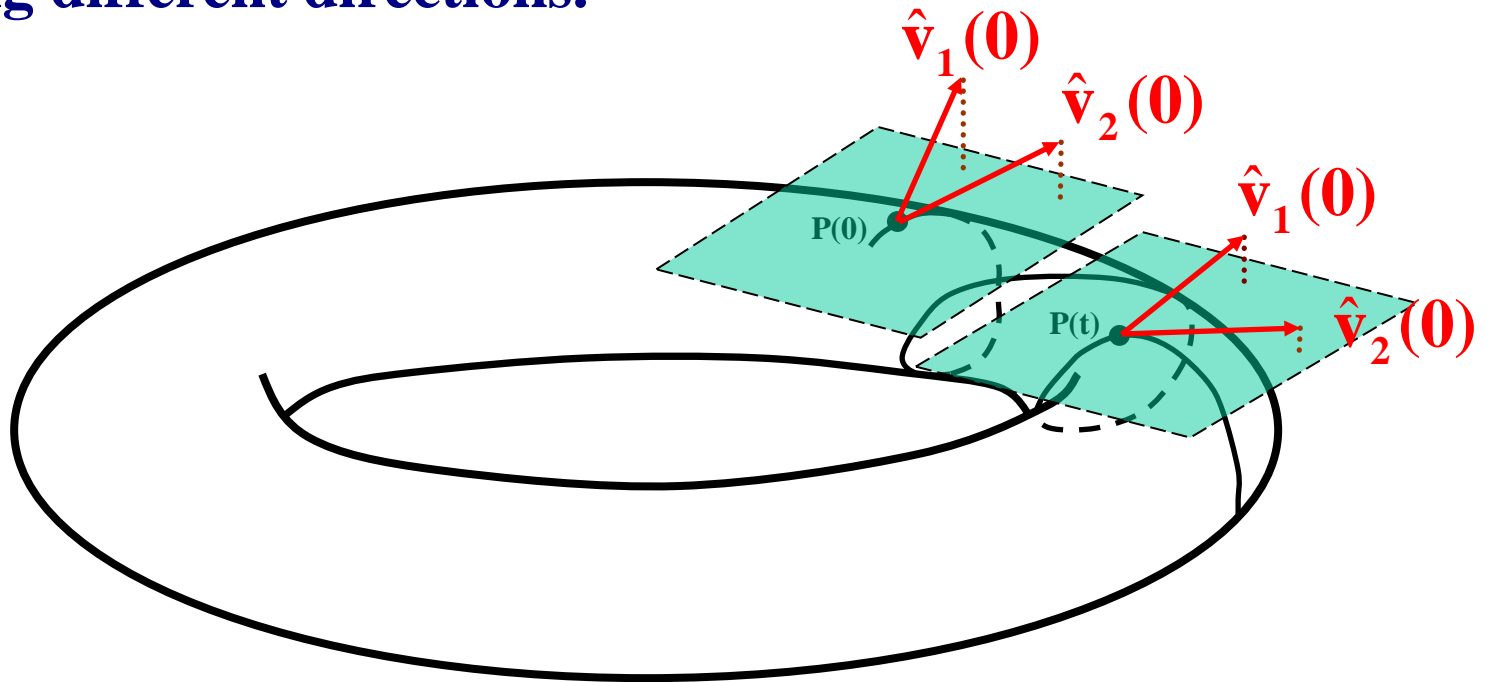
Behavior of SALI for regular motion

Regular motion occurs on a torus and two different initial deviation vectors become tangent to the torus, generally having different directions.



Behavior of SALI for regular motion

Regular motion occurs on a torus and two different initial deviation vectors become tangent to the torus, generally having different directions.



SALI – Hénon-Heiles system

As an example, we consider the 2D Hénon-Heiles system:

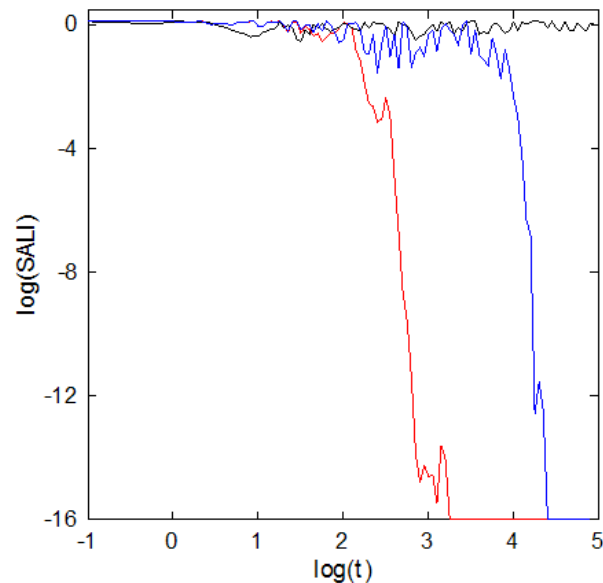
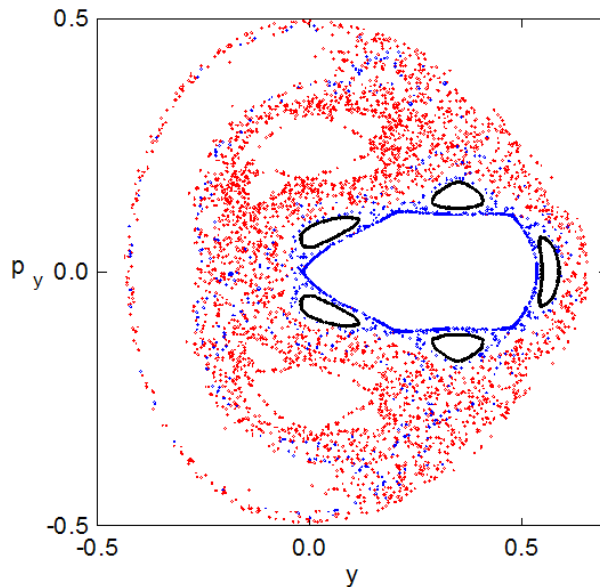
$$H = \frac{1}{2}(p_x^2 + p_y^2) + \frac{1}{2}(x^2 + y^2) + x^2y - \frac{1}{3}y^3$$

For $E=1/8$ we consider the orbits with initial conditions:

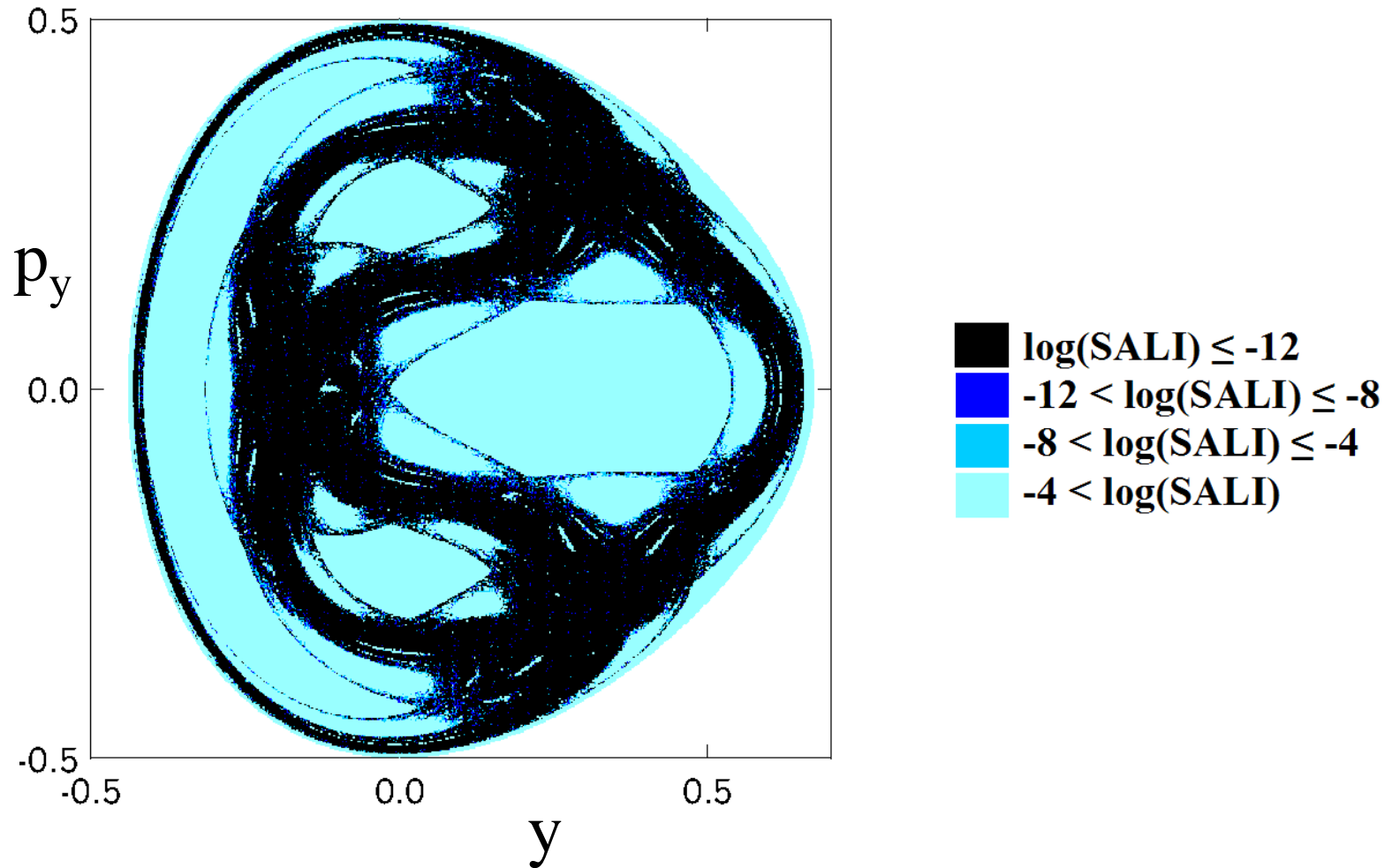
Regular orbit, $x=0$, $y=0.55$, $p_x=0.2417$, $p_y=0$

Chaotic orbit, $x=0$, $y=-0.016$, $p_x=0.49974$, $p_y=0$

Chaotic orbit, $x=0$, $y=-0.01344$, $p_x=0.49982$, $p_y=0$



SALI – Hénon-Heiles system



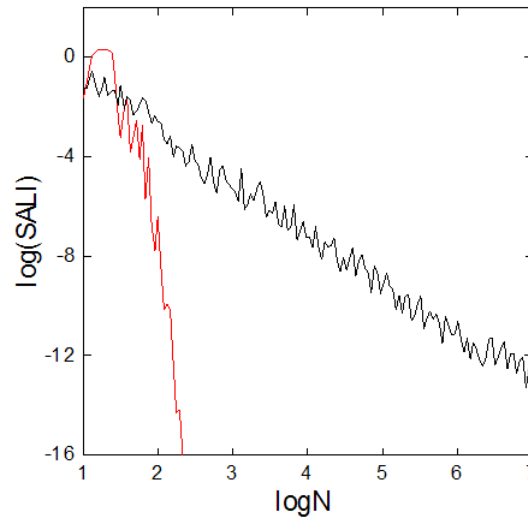
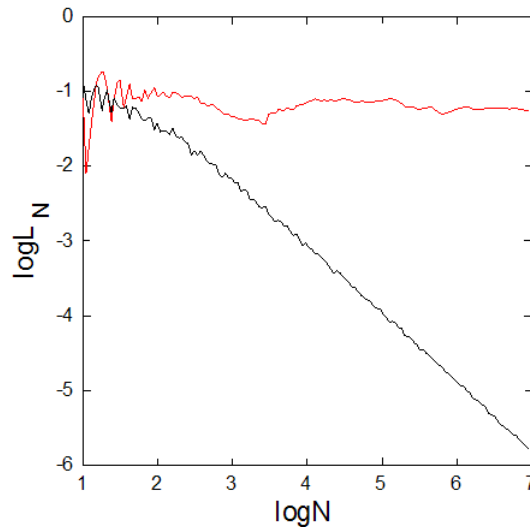
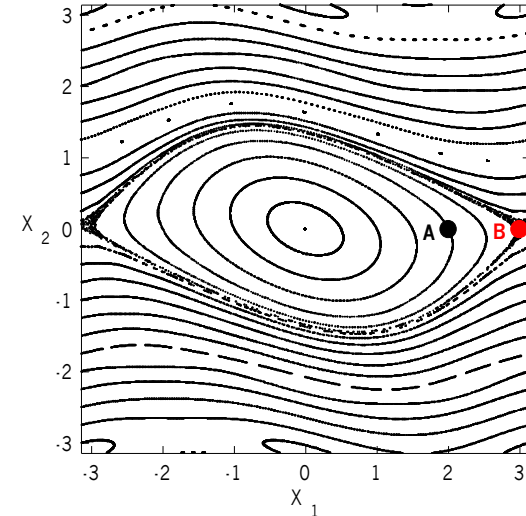
Applications – 2D map

$$\begin{aligned} \mathbf{x}'_1 &= \mathbf{x}_1 + \mathbf{x}_2 \\ \mathbf{x}'_2 &= \mathbf{x}_2 - \nu \sin(\mathbf{x}_1 + \mathbf{x}_2) \end{aligned} \quad (\text{mod } 2\pi)$$

For $\nu=0.5$ we consider the orbits:

regular orbit A with initial conditions $x_1=2, x_2=0$.

chaotic orbit B with initial conditions $x_1=3, x_2=0$.



Behavior of the SALI

2D maps

SALI $\rightarrow 0$ both for regular and chaotic orbits

following, however, completely different time rates which allows us to distinguish between the two cases.

Hamiltonian flows and multidimensional maps

SALI $\rightarrow 0$ for chaotic orbits

SALI \rightarrow constant $\neq 0$ for regular orbits

Using LDs to quantify chaos

We consider orbits on a finite grid of an $n(\geq 1)$ -dimensional subspace of the $N(\geq n)$ -dimensional phase space of a dynamical system and their LDs.

Any non-boundary point x in this subspace has $2n$ nearest neighbors

$$y_i^\pm = x \pm \sigma^{(i)} e^{(i)}, \quad i = 1, 2, \dots, n,$$

where $e^{(i)}$ is the i th usual basis vector in \mathbb{R}^n and $\sigma^{(i)}$ is the distance between successive grid points in this direction.

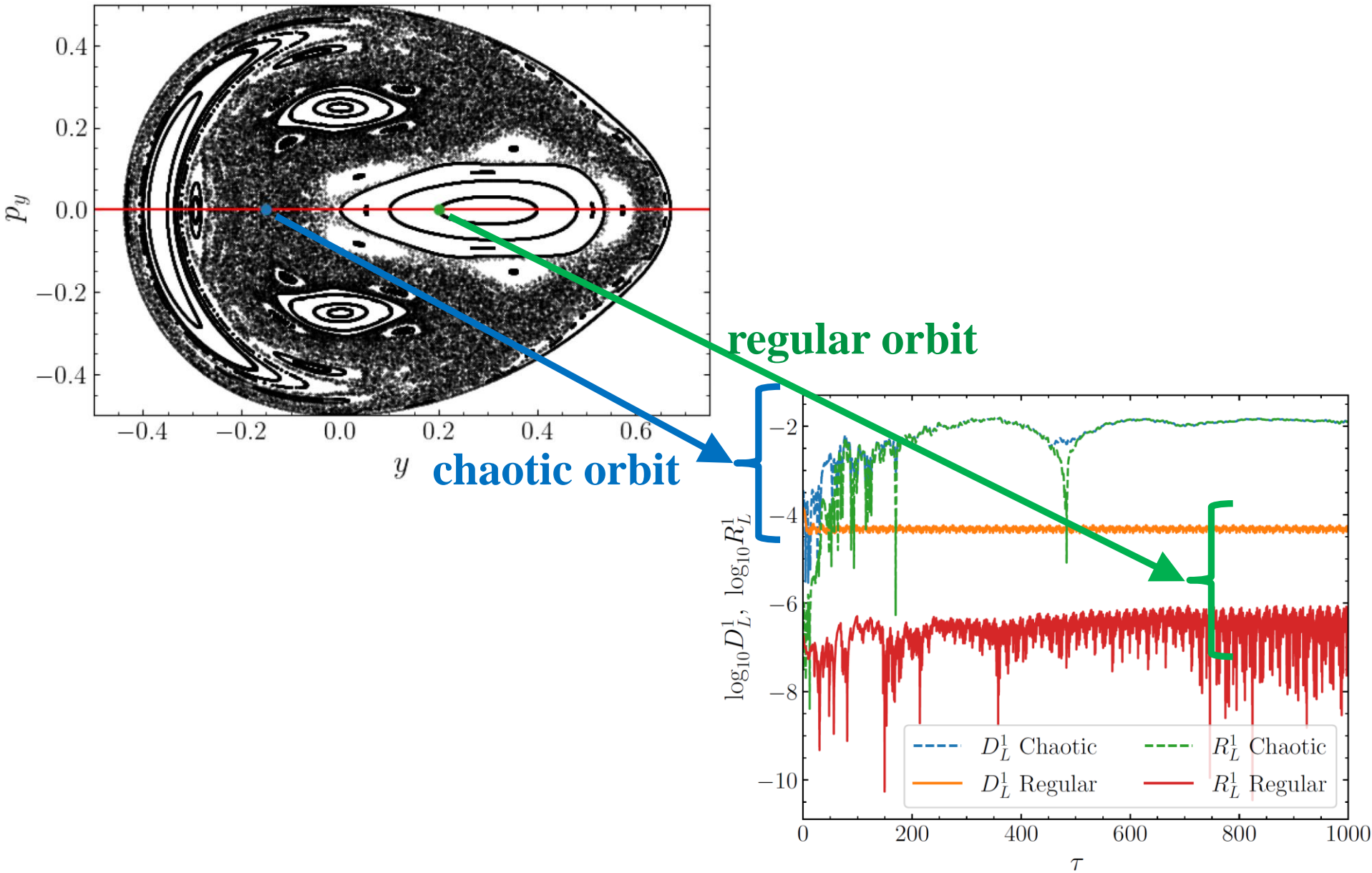
The **difference** D_L^n of neighboring orbits' LDs:

$$D_L^n(x) = \frac{1}{2n} \sum_{i=1}^n \frac{|LD^f(x) - LD^f(y_i^+)| + |LD^f(x) - LD^f(y_i^-)|}{LD^f(x)}.$$

The **ratio** R_L^n of neighboring orbits' LDs:

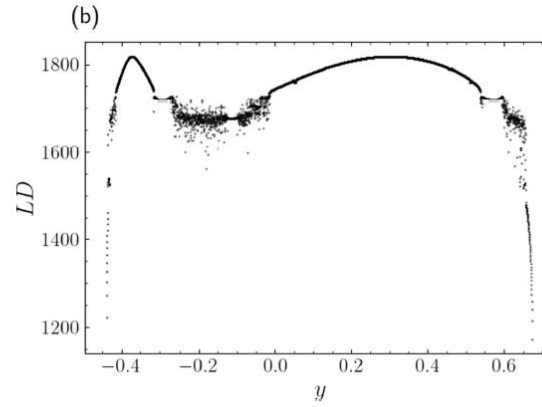
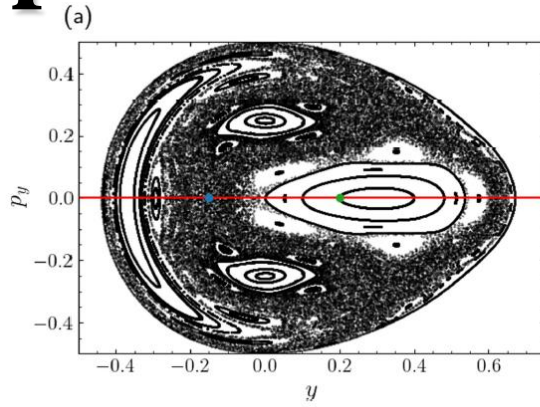
$$R_L^n(x) = \left| 1 - \frac{1}{2n} \sum_{i=1}^n \frac{LD^f(y_i^+) + LD^f(y_i^-)}{LD^f(x)} \right|.$$

Application: Hénon-Heiles system



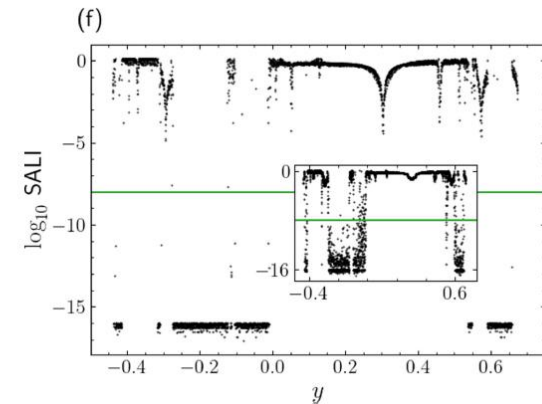
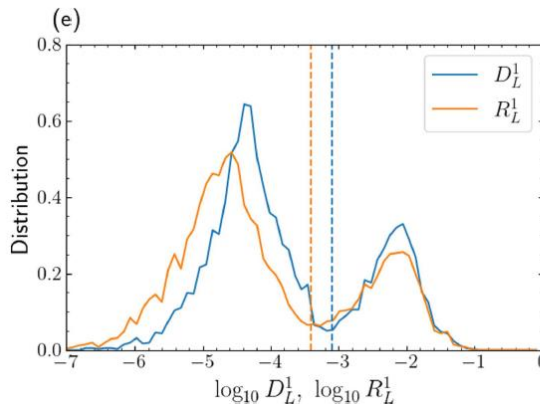
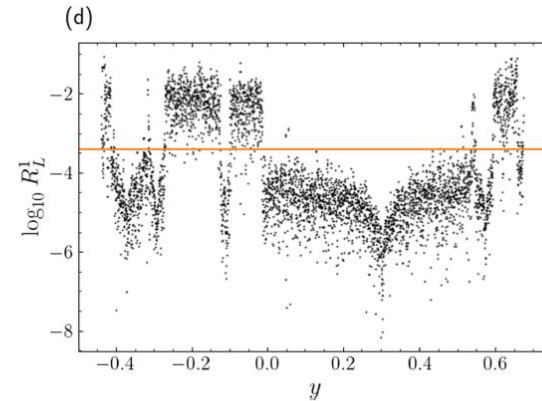
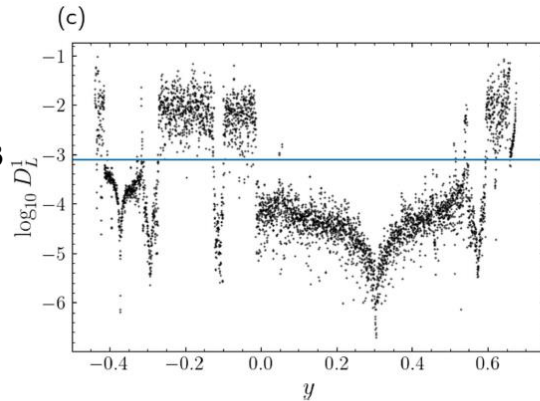
Application: Hénon-Heiles system

$H=1/8$



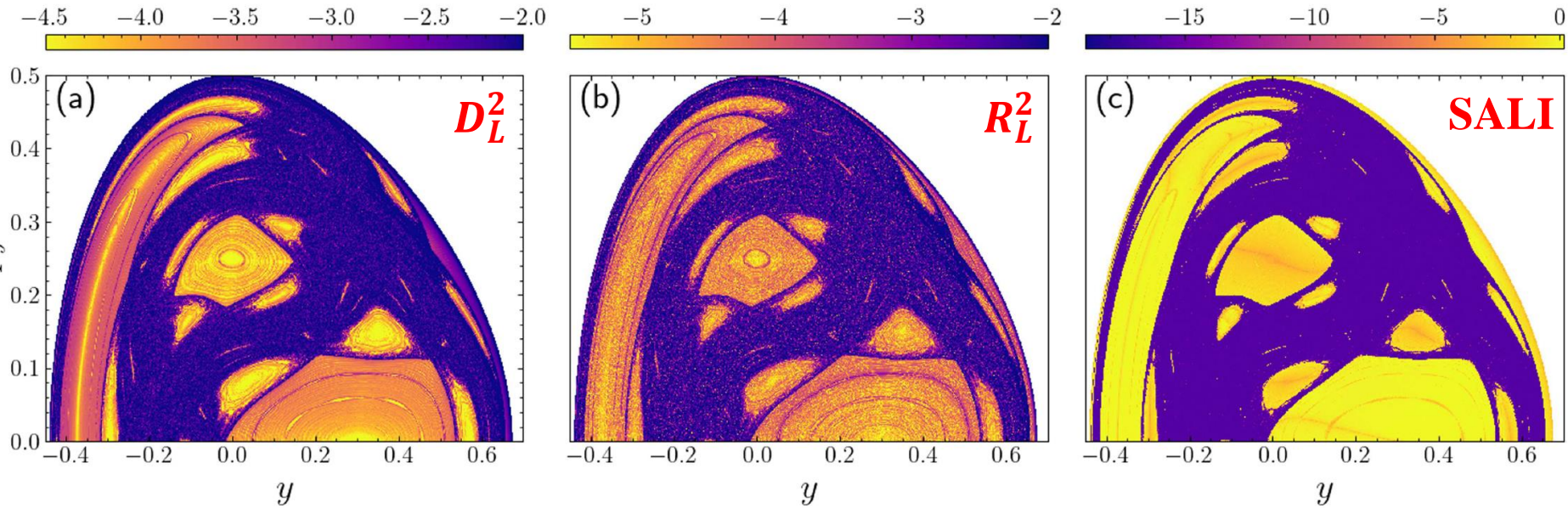
Variation of LDs with regard to initial conditions.
regular regions: smooth
chaotic regions: erratic
[also see Montes et al., Commun. Nonlin. Sci. Num. Simul. (2021)]

LDs for $\tau=10^3$

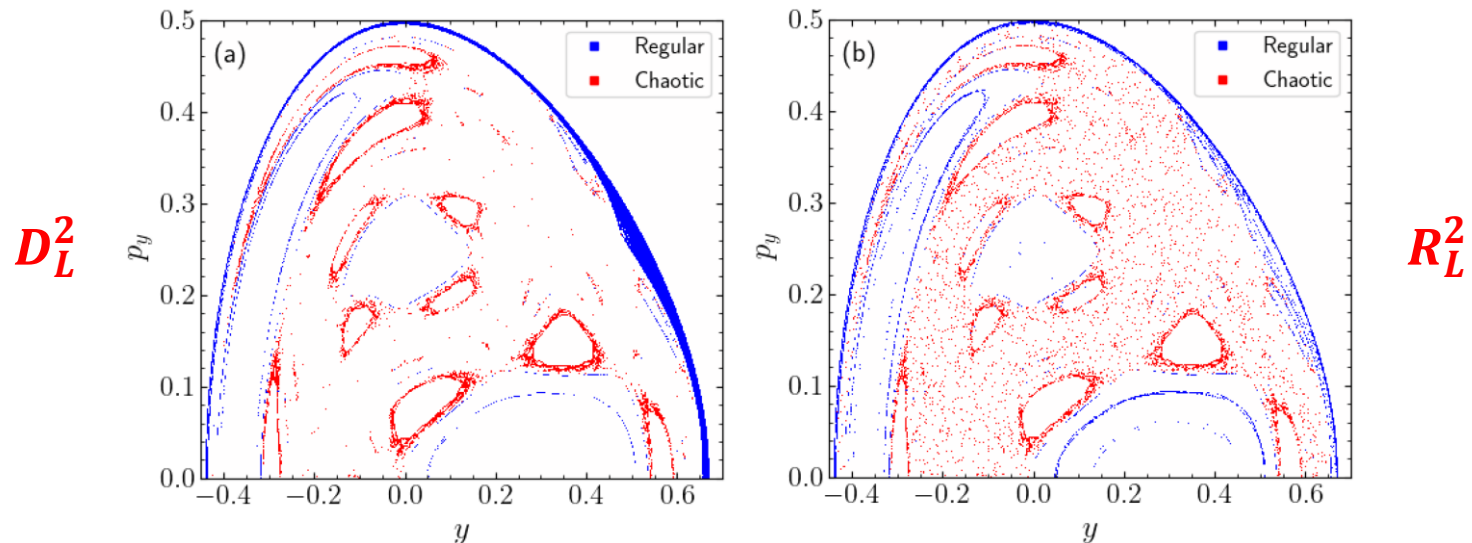


SALI for $\tau=10^6$
(inset $\tau=10^3$)

Application: Hénon-Heiles system



Misclassified orbits (< 10%)

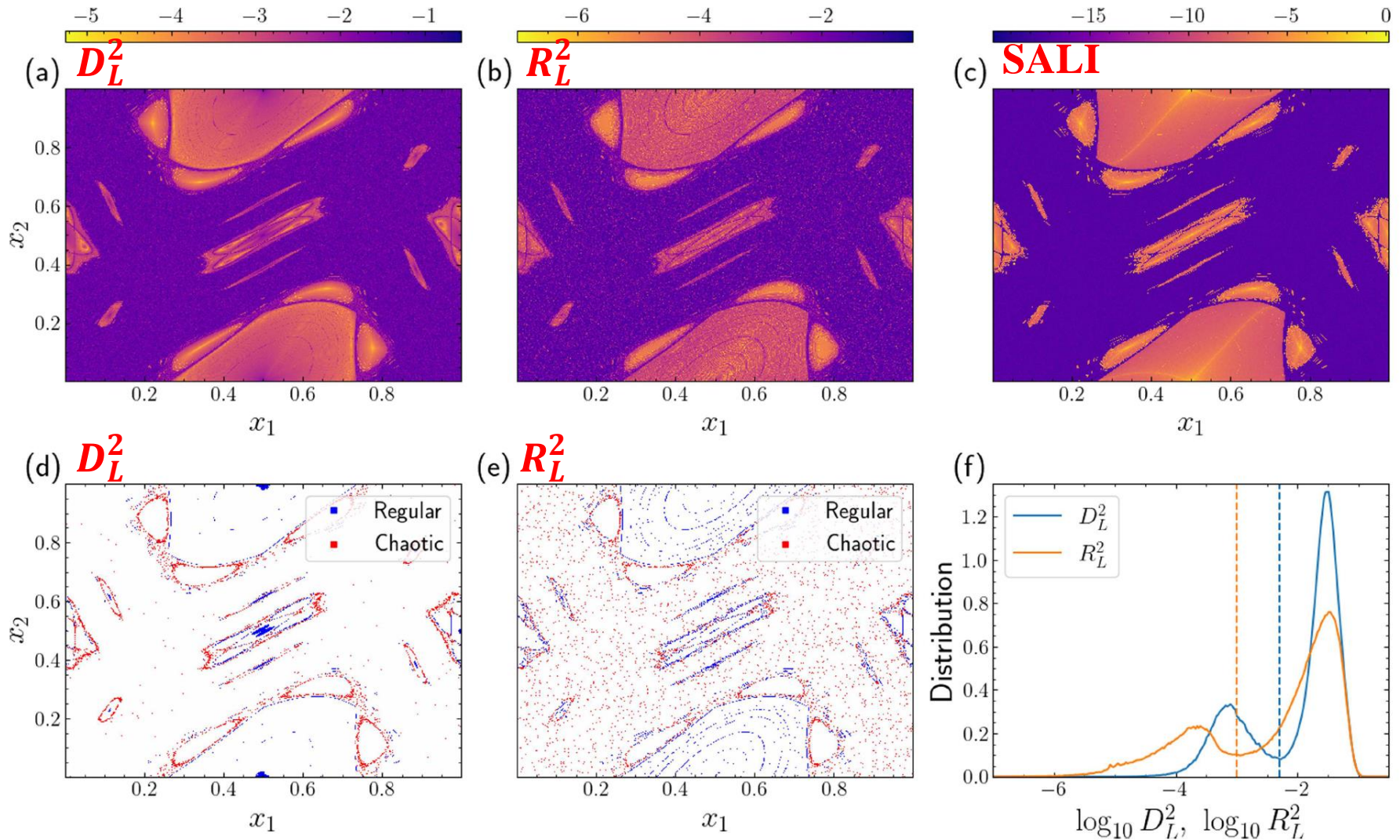


Application: 2D Standard map

We set $K = 1.5$

$$\begin{aligned}x'_1 &= x_1 + x'_2 \\x'_2 &= x_2 + \frac{K}{2\pi} \sin(2\pi x_1) \pmod{1}\end{aligned}$$

Thresholds: $\log_{10} D_L^2 = -2.3$, $\log_{10} R_L^2 = -3$ ($T = 10^3$)
 $\log_{10} \text{SALI} = -12$ ($T = 10^5$)



Effect of grid spacing (σ) and final integration time (T, τ)

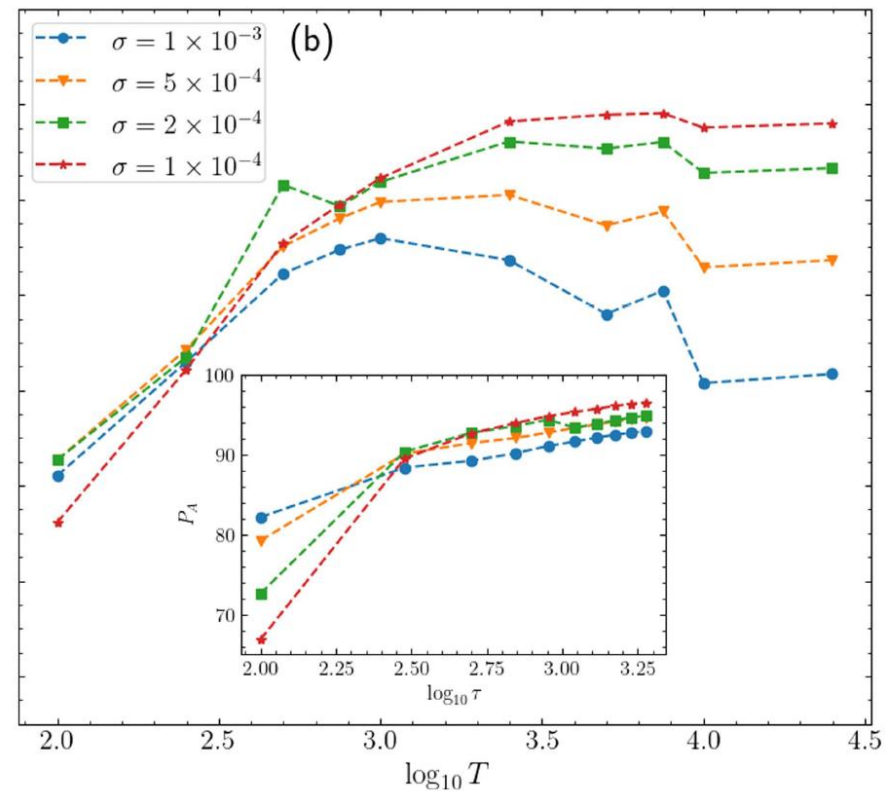
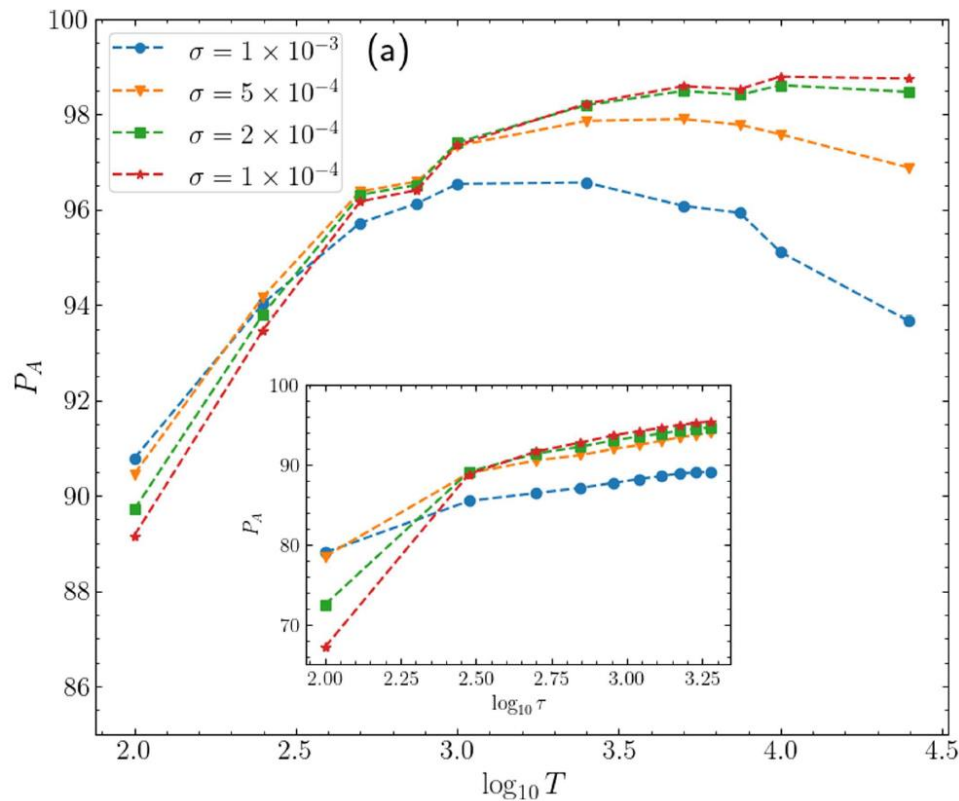
P_A : percentage of correctly characterized orbits

Main plots: 2D Standard map

Insets: Hénon-Heiles system

D_L^2

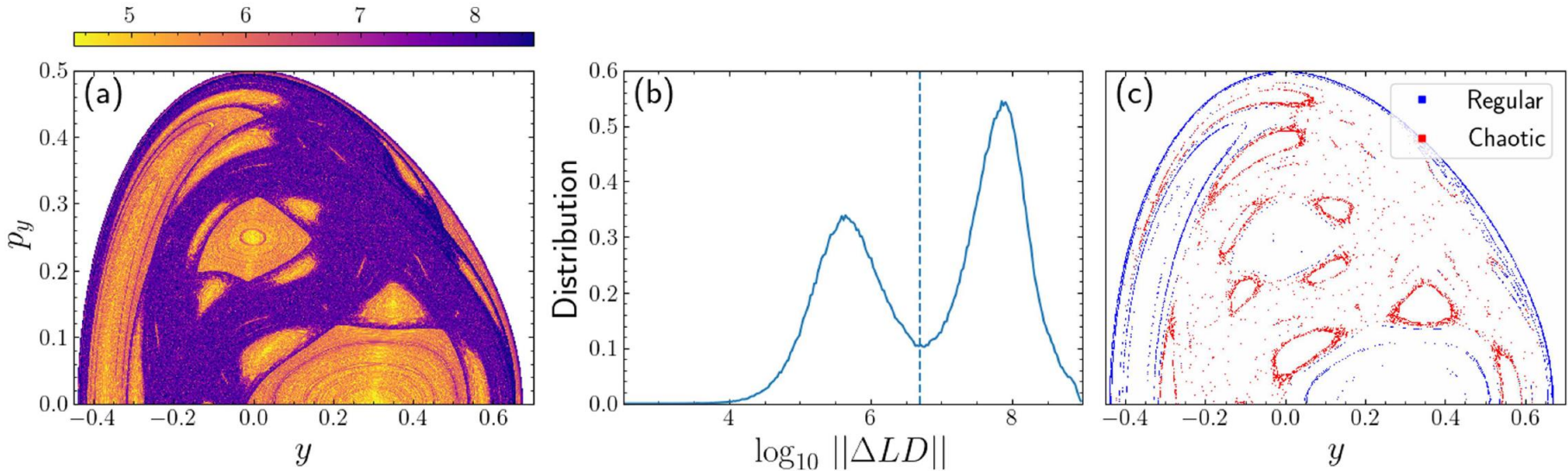
R_L^2



Application: Hénon-Heiles system

A quantity related to **the second spatial derivative of the LDs** was introduced in Daquin et al., Physica D (2022) and was used in Hillebrand et al., Chaos (2022):

$$\|\Delta LD\|(x) = \left| \frac{LD^f(y_i^+) - 2LD^f(x) + LD^f(y_i^-)}{\sigma^2} \right|.$$

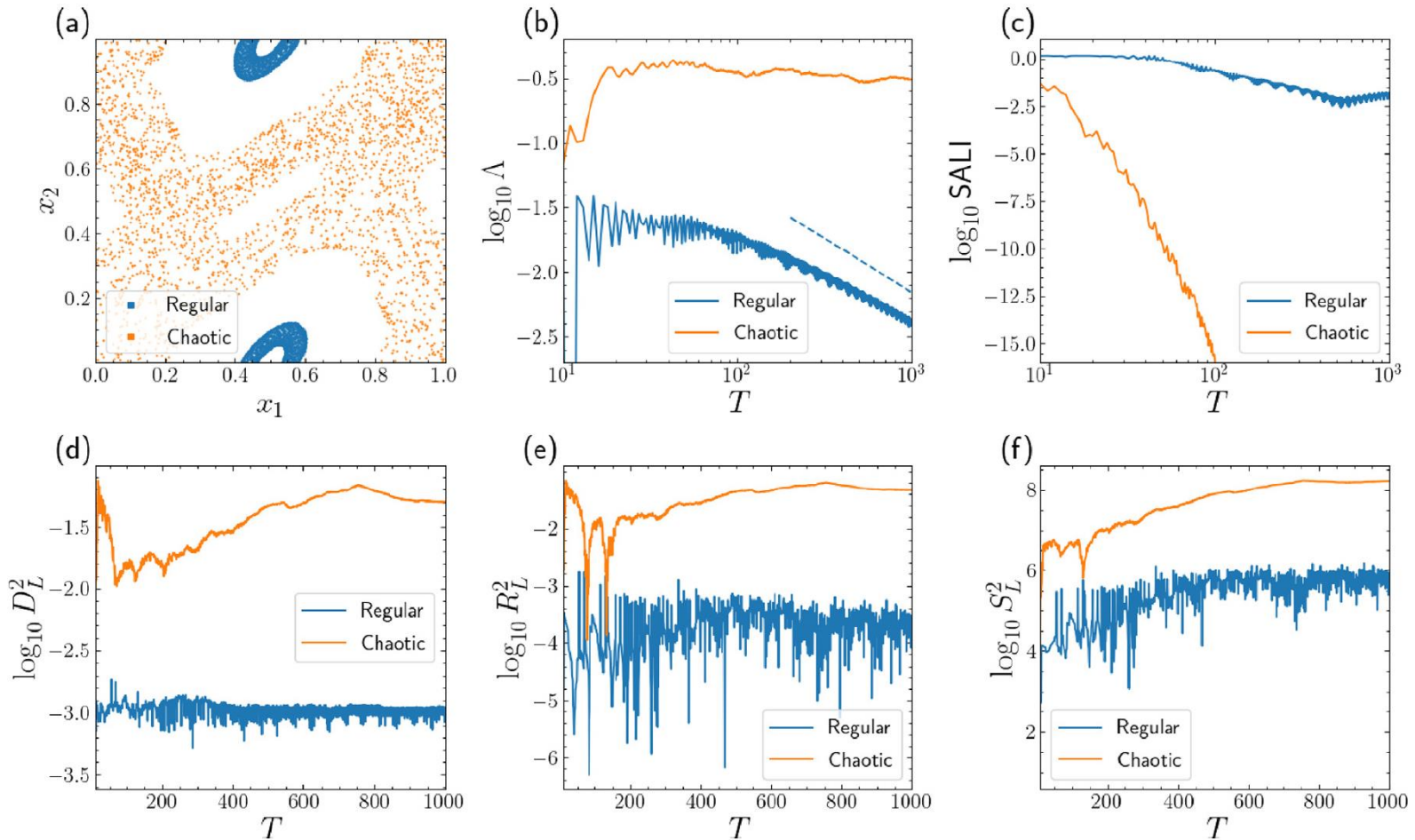


In Zimmer et al., Physica D (2023) it was modified to:

$$S_L^n(x) = \frac{1}{n} \sum_{i=1}^n \left| \frac{LD^f(y_i^+) - 2LD^f(x) + LD^f(y_i^-)}{(\sigma^{(i)})^2} \right|.$$

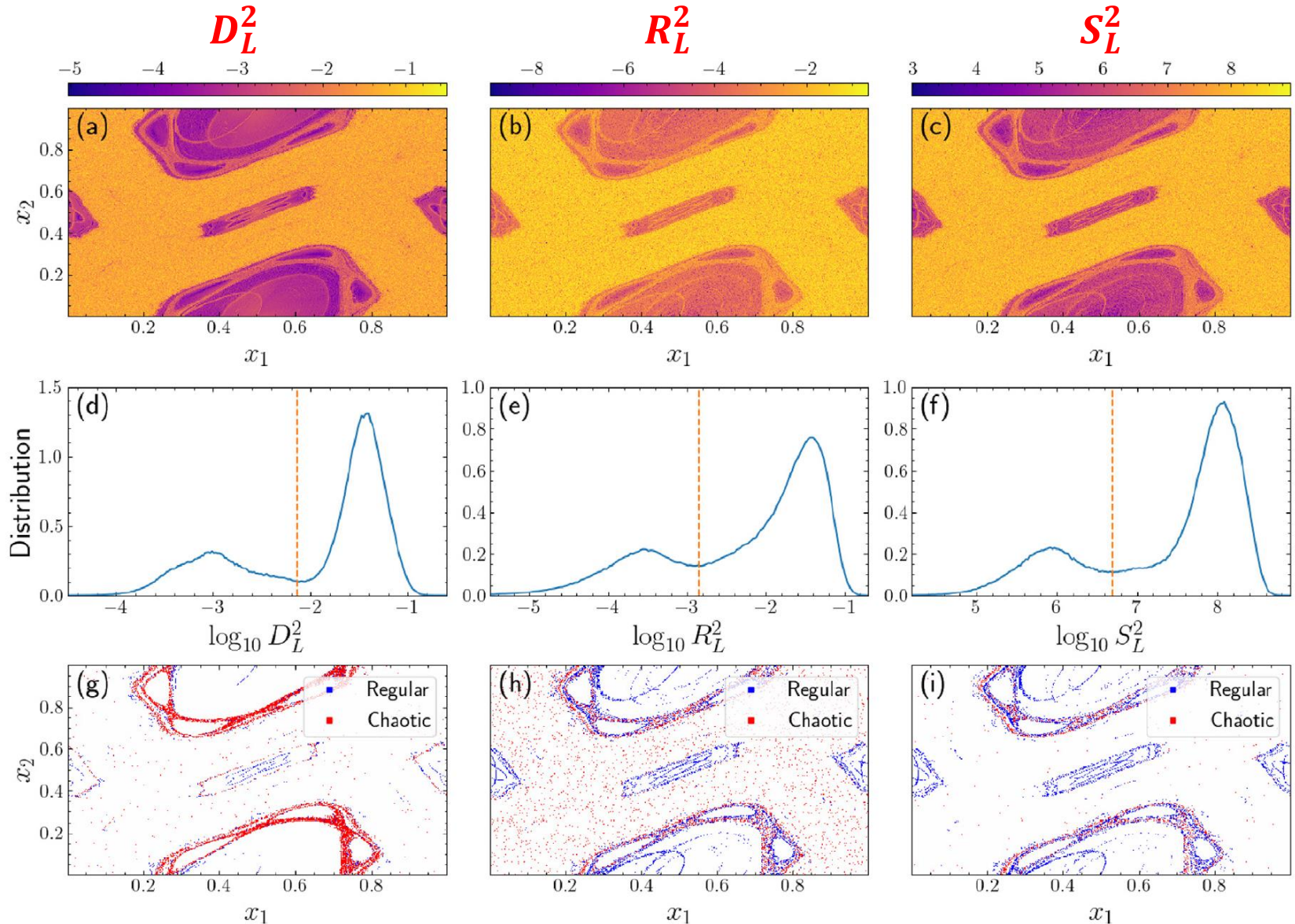
Application: 4D Standard map

$$\begin{aligned}x'_1 &= x_1 + x'_2 \\x'_2 &= x_2 + \frac{K}{2\pi} \sin(2\pi x_1) - \frac{B}{2\pi} \sin[2\pi(x_3 - x_1)] \\x'_3 &= x_3 + x'_4 \\x'_4 &= x_4 + \frac{K}{2\pi} \sin(2\pi x_3) - \frac{B}{2\pi} \sin[2\pi(x_1 - x_3)]\end{aligned} \quad (\text{mod } 1)$$



Application: 4D Standard map

2D subspace (x_1, x_2) with $x_3 = 0.54$, $x_4 = 0.01$ for $K = 1.5$, $B = 0.05$ and $T = 10^3$



Summary

- ✓ We introduced and successfully implemented computationally efficient ways to **effectively identify chaos** in conservative dynamical systems **from the values of LDs at neighboring initial conditions.**
- ✓ From the distributions of the indices' values we determine appropriate **threshold values**, which allow the characterization of orbits as regular or chaotic.
- ✓ All indices **faced problems** in correctly revealing the nature of some orbits mainly **at the borders of stability islands.**
- ✓ All indices show **overall very good performance**, as their classifications are in accordance with the ones obtained by **the SALI** (which is a very efficient and accurate chaos indicator) at a level of at least **90% agreement.**
- ✓ **Advantages:**
 - **Easy to compute** (actually only the forward LDs are needed).
 - **No need to know and to integrate the variational equations.**

References

- Madrid & Mancho, *Chaos*, **19**, 013111 (2009)
- Mendoza & Mancho, *PRL*, **105**, 038501 (2010)
- Mancho, Wiggins, Curbelo & Mendoza, *Commun. Nonlin. Sci. Num. Simul.*, **18**, 3530 (2013)
- Lopesino, Balibrea, Wiggins & Mancho, *Commun. Nonlin. Sci. Num. Simul.*, **27**, 40 (2015)
- Lopesino, Balibrea-Iniesta, García-Garrido, Wiggins & Mancho, *Int. J. Bifurc. Chaos*, **27**, 1730001 (2017)
- Agaoglou, Aguilar-Sanjuan, García-Garrido, González-Montoya, Katsanikas, Krajňák, Naik & Wiggins, ‘Lagrangian descriptors: Discovery and quantification of phase space structure and transport’, <https://doi.org/10.5281/zenodo.3958985> (2020)
- Montes, Revuelta & Borondo, *Commun. Nonlin. Sci. Num. Simul.*, **102**, 105860 (2021)
- Daquin, Pédenon-Orlanducci, Agaoglou, García-Sánchez & Mancho, *Physica D*, **442**, 133520 (2022)
- S., *J. Phys. A*, **34**, 10029 (2001)
- S., Antonopoulos, Bountis & Vrahatis, *J. Phys. A*, **37**, 6269 (2004)
- S. & Manos, *Lect. Notes Phys.*, **915**, 129 (2016)

Hillebrand, Zimper, Ngapasare, Katsanikas, Wiggins & S.: *Chaos*, **32**, 123122 (2022),
‘Quantifying chaos using Lagrangian descriptors’

Zimper, Ngapasare, Hillebrand, Katsanikas, Wiggins & S.: *Physica D*, **453**, 133833 (2023),
‘Performance of chaos diagnostics based on Lagrangian descriptors. Application to the 4D standard map’